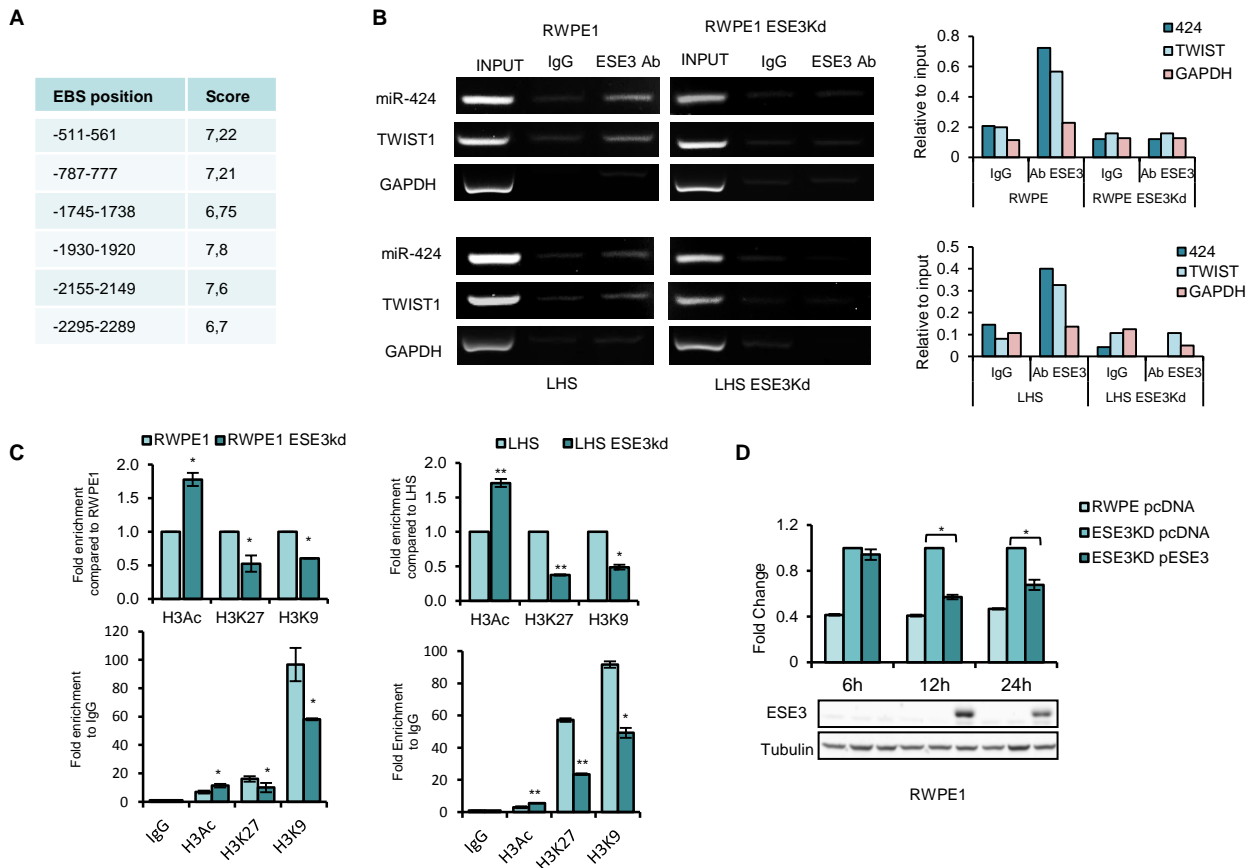
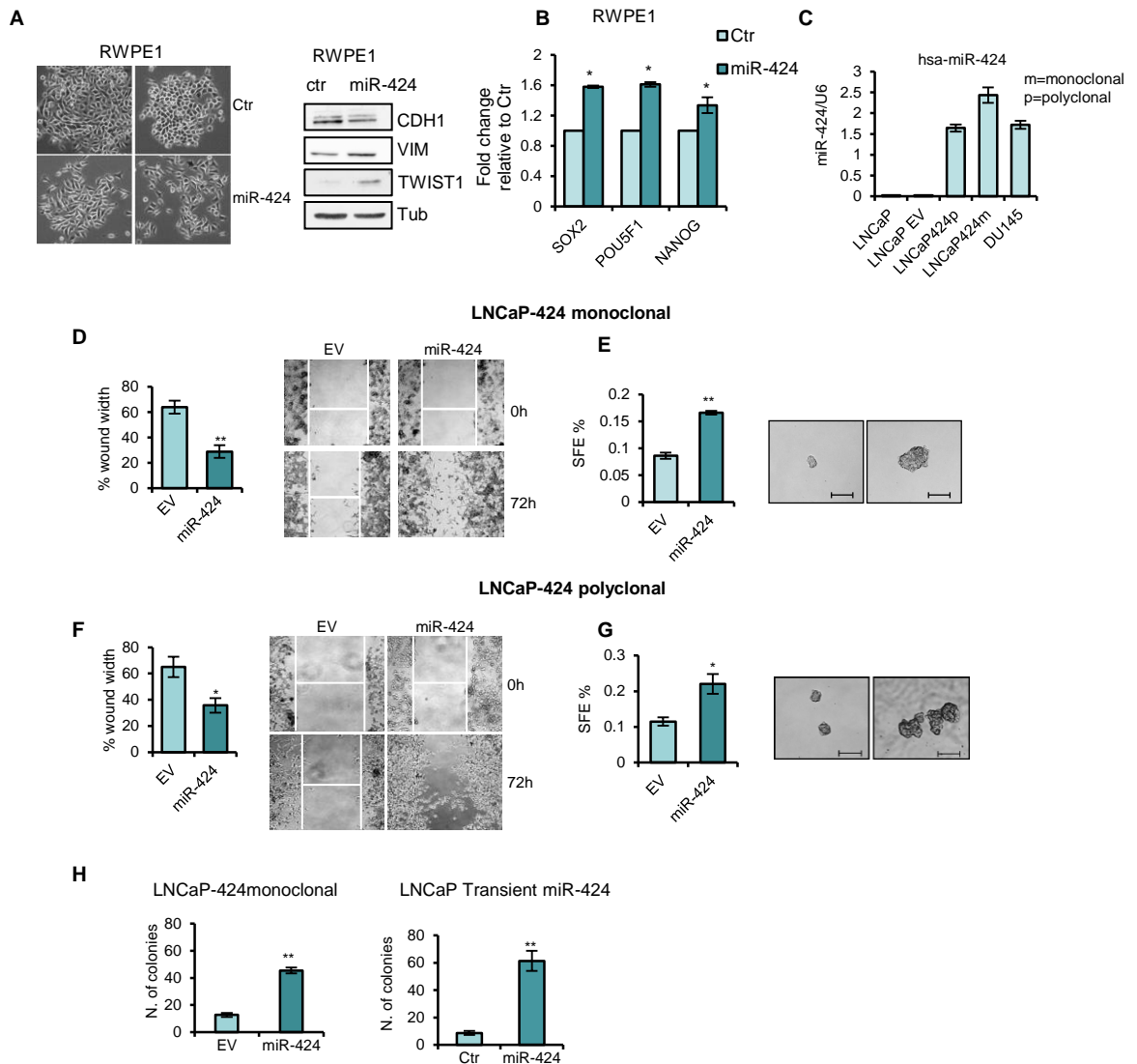


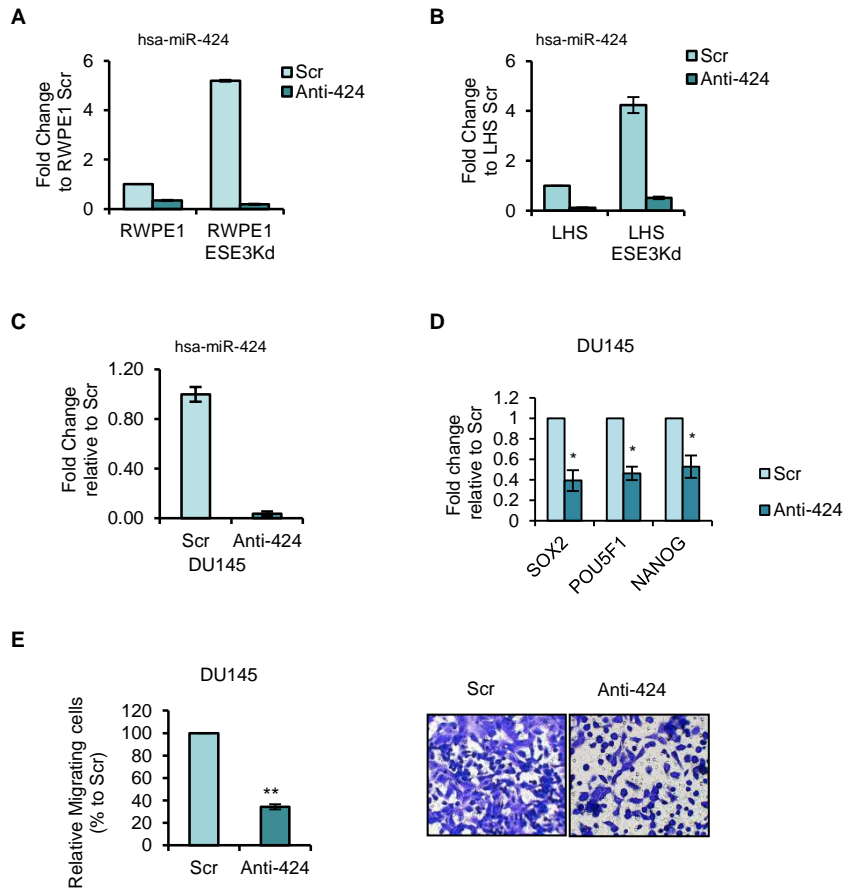
Supplementary Figure 1. miR-424 is upregulated in ERG negative tumors and associated with aggressive features. (A) miR-424 log₂ intensity levels evaluated by microarray in Normal and Prostate tumors. p-value is indicated (B) Percentage of ERG positive tumors among miR-424 high and miR-424 low tumors in TCGA and BIELLA cohorts. (C) miR-424 (left) and ESE3 (right) level evaluated by microarray in indicated cell lines. (D) AR scores of prostate tumors divided according to their level of miR-424 in the TCGA dataset. (E) miR-424 level evaluated by microarray in indicated tumour datasets. p values of modified t-test are indicated.



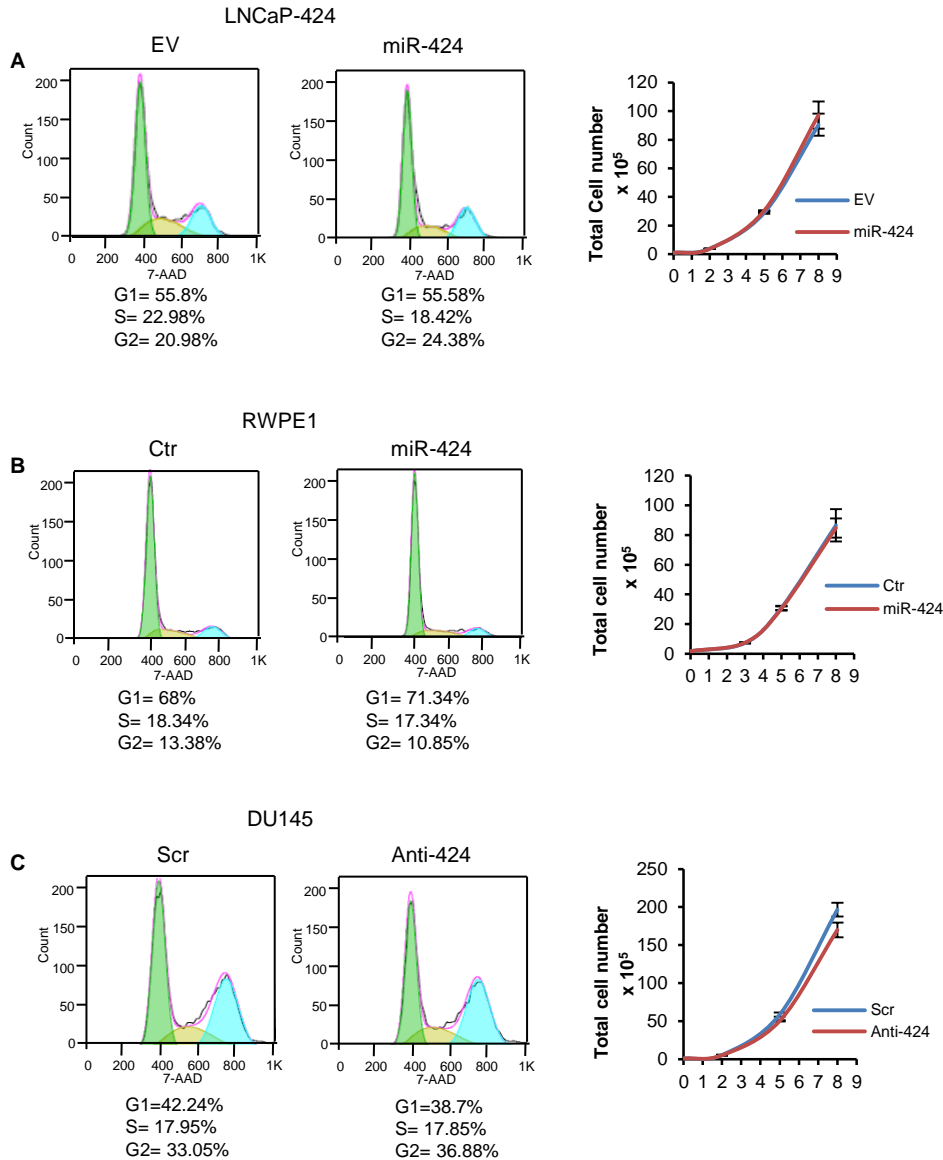
Supplementary Figure 2. ESE3/EHF occupies miR-424 promoter region and represses miR-424 transcription. (A) Position and scores of ETS binding sites evaluated on miR-424 promoter and identified using *MotifViz* (B) ESE3 occupancy on TWIST1 promoter and GAPDH promoter evaluated by end point PCR as positive control and negative control, respectively. (C) *Top panels*, Histone 3 acetylation (H3Ac), lysine 27 and lysine 9 methylation (H3K27 and H3K9) occupancy on miR-424 promoter evaluated by ChIP in indicated cell lines. The results were normalized on IgG and represented as fold enrichment relative to the parental cell line. *Lower panels*, ChIP data presented as fold enrichment relative to IgG. (D) miR-424 level evaluated by qRT-PCR in RWPE1 control (CTR) and ESE3Kd cells following ectopic expression of ESE3 (pESE3) or control vector (pcDNA) at the indicated time points. *Lower panel*, Immunoblot of ESE3/EHF at indicated time points following overexpression of pESE3 (*lower*). The values are normalized to RNU6 and represented as miR-424 expression relative to pcDNA transfected RWPE1 ESE3Kd cells. Data show mean \pm s.d. (n=3). * $p \leq 0.05$ ** $p \leq 0.01$ by two-tailed Student's t-test. n.s, not significant.



Supplementary Figure 3. Transient and stable expression of miR-424 sustains malignant phenotypes in multiple cell models. (A) Phase-contrast pictures showing cell morphology (*left*) and western blot for indicated EMT markers (*right*) (B) Expression of CSCs markers evaluated in RWPE1 72h following miR-424 overexpression. (C) Level of miR-424 evaluated by qRT-PCR in indicated cell lines. (D-E), cell migration by WH (D), SFE and representative images of spheroids (E) evaluated in LNCaP-424 monoclonal cells. Empty-vector (EV). (F-G), cell migration by WH (F), SFE and representative images of spheroids (G) evaluated in LNCaP-424 polyclonal cells. Empty-vector (EV). (H) Colony formation in soft agar in LNCaP-424 monoclonal cells (*left*) and following transient transfection of miR-424 precursor (miR-424) or negative control (Ctr) in LNCaP cells (*right*). Data show mean \pm s.d. (n=3). * $p \leq 0.05$ ** $p \leq 0.01$ by two-tailed Student's t-test. Scale bars: 200 μ m



Supplementary Fig. 4. miR-424 induces CSCs markers. (A-C) miR-424 level evaluated by qRT-PCR 24 h following transfection of anti-miR-424 in the indicated cell lines. The miRNA level was normalized to RNU6 and represented as fold change relative to the indicated Scr control. (D) Expression of CSCs markers in DU145 cells 72h following anti-miR-424 transfection. (E) Cell migration and invasion by the Boyden chamber assay following anti-miR-424 transfection. Percentage of invading cells (*left*) and images of invading cells (*right*). The assay was done in triplicate and the value represent the mean \pm s.d. of two independent experiments.

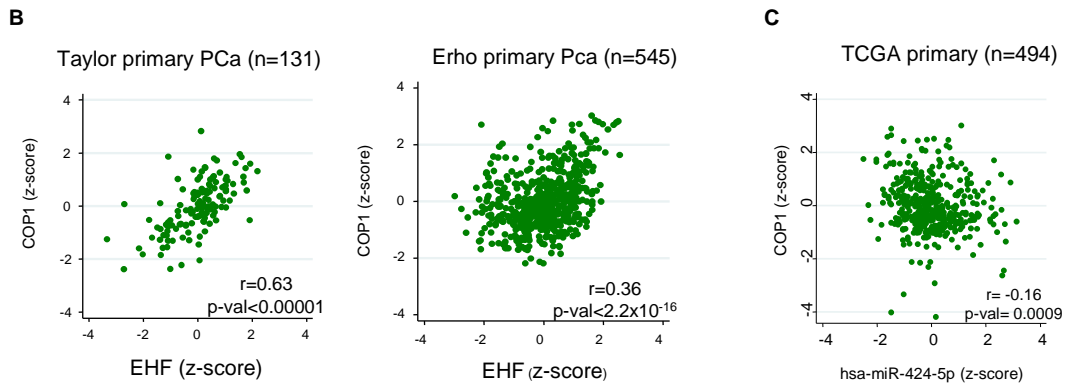


Supplementary Figure 5. miR-424 does not affect cell cycle and cell proliferation in vitro.

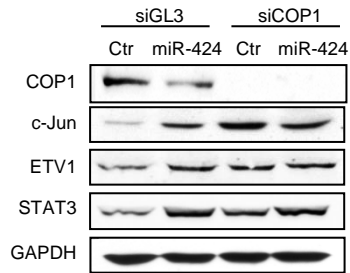
(A-C) Cell cycle analysis by 7AAD staining (*left panels*) and cell proliferation assay (*right panels*) were performed in LNCaP-424 monoclonal cell line (A) and RWPE1 cells (B) following miR-424 overexpression and in DU145 cells (C) following miR-424 inhibition by anti-miR-424. Cell cycle analysis were performed 72h after cell seeding or transfection and percentage of cells in G1, S and G2 are indicated. Cell counts for cell proliferation assay were done at the indicated time points up to 8 days following cell seeding.

A EHF/RFWD2/COP1 POSITIVE CORRELATION IN EPITHELIAL TUMORS

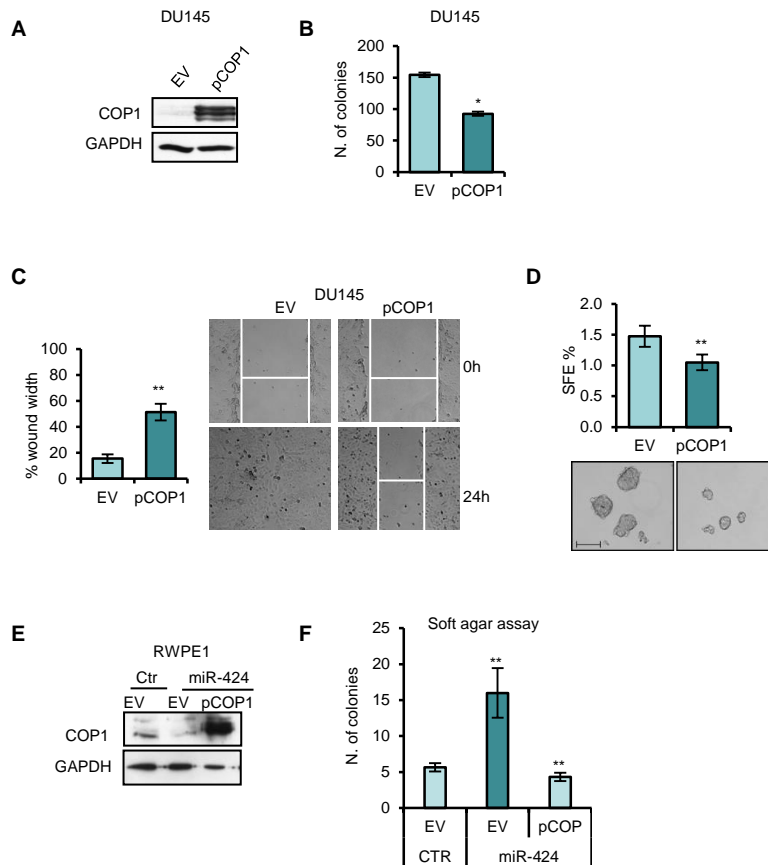
	correlation (pearson r)	significance (p-val)
Primary prostate cancer		
Chandran (n=10)	0.87	0.0012
Taylor (n=131)	0.63	<0.00001
Gulzar (n=72)	0.43	0.0004
Erho (n=545)	0.36	<2x10 ⁻¹⁶
Grasso (n=59)	0.30	0.020
Prostate cancer metastasis		
Chandran (n=21)	0.48	0.029
Other tumors (Pancancer study)		
Kidney Papillary Cell Carcinoma (n=161)	0.22	0.0052
Breast (n=991)	0.20	<0.00001
Kidney Clear Cell Carcinoma (n=506)	0.19	<0.00001
Thyroid Cancer (n=492)	0.17	0.0001
Bladder (n=211)	0.16	0.017



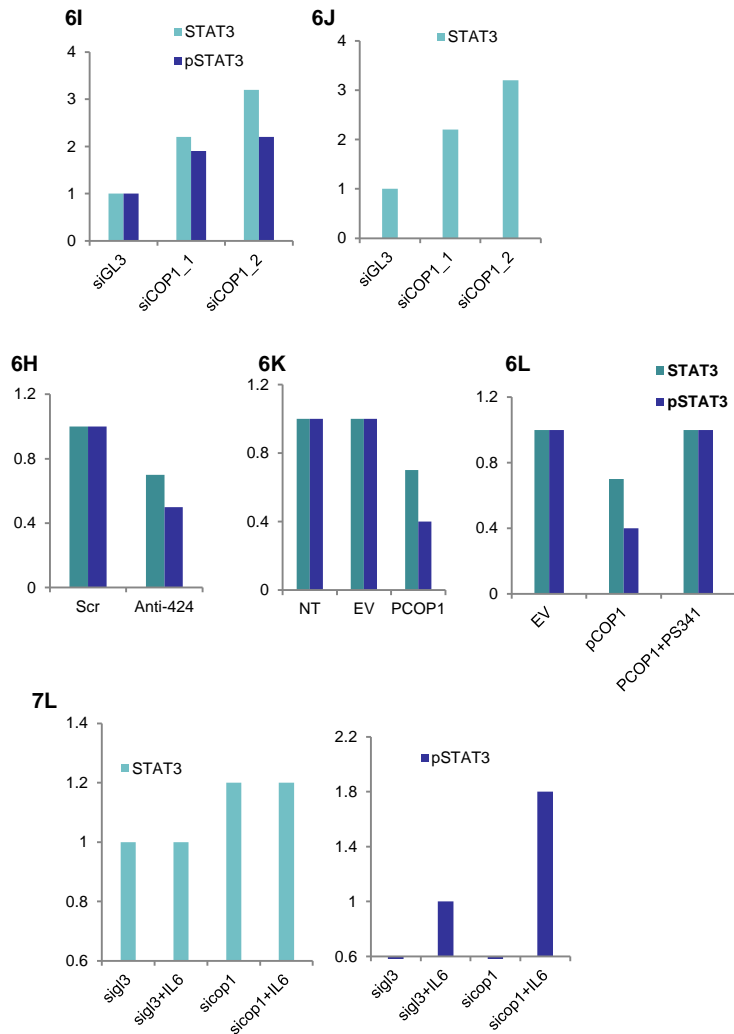
Supplementary Figure 6. ESE3/EHF and RFWD2/COP1 are correlated in prostate tumours. (A) Pearson correlation analysis showing positive correlation between ESE3/EHF and RFWD2/COP1 mRNA in multiple epithelial cancers. (B) Correlation plots in Taylor and Erho datasets. Pearson value and significance are indicated. (C) Pearson distribution plot showing significant inverse correlation between miR-424 and RFWD2/COP1 mRNA level in primary prostate tumours TCGA dataset) ($r=-0.16$; $p<0.0009$). (see Material and Methods for further details).



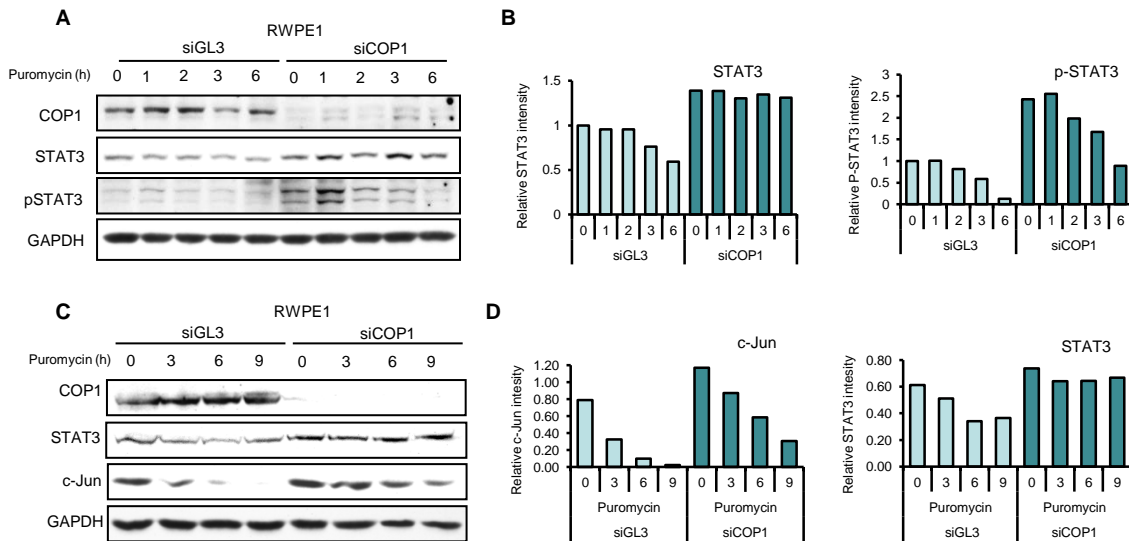
Supplementary Figure 7. miR-424 acts through COP1 repression. Immunoblot for c-Jun, ETV1, STAT3 and COP1 in RWPE cells 48h following co-transfection with siRNA against COP1 or control siRNA (siGL3) and pre-miR424 or Ctr.



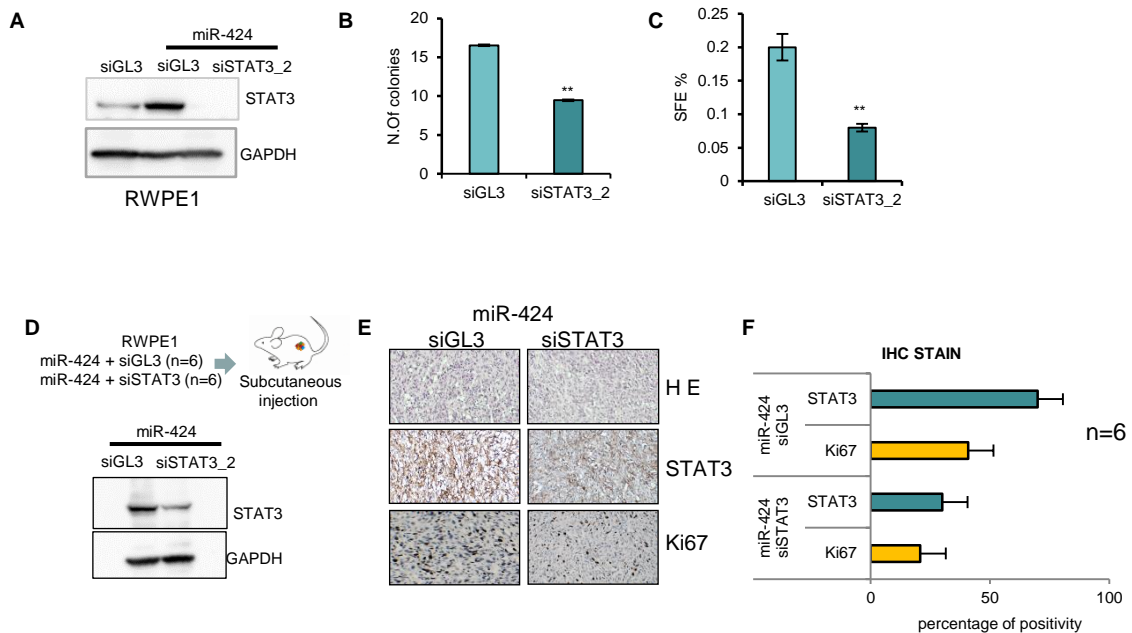
Supplementary Figure 8. COP1 overexpression reverts malignant phenotypes in DU145 prostate cancer cells and the oncogenic effects of miR-424 in normal prostate epithelial cells. (A-D) Immunoblot of COP1 (A), colony formation in soft agar (B), cell migration by WH (C) and SFE and representative images of spheroid (D) following transfection of FLAG-COP1 (pCOP1) or Empty-vector (EV) in DU145 cells. (E) Immunoblot of COP1 following transfection of FLAG-COP1 (pCOP1) or Empty-vector (EV) along with control and miR-424 in RWPE1 cells. (F) Colony formation in soft agar in RWPE1 transfected as described in E. Data shown mean \pm s.d. (n=3) of one representative experiment. * $p \leq 0.05$ ** $p \leq 0.01$ by two-tailed Student's t-test.



Supplementary Figure 9. Densitometric analysis of western-blot related to figures 6I,6J,6H,6K 6L and 7L.



Supplementary Figure 10. COP1 induces STAT3 ubiquitination and degradation. (A-C) IB of indicated protein in RWPE1 cells transfected with siCOP1#1 or siGL3 and treated with puromycin (50 μ M) for the indicated time points. c-Jun and GAPDH were evaluated as controls (B-D). Densitometric analysis relative to STAT3, p-STAT3 and c-Jun bands are shown .



Supplementary Figure 11. STAT3 ablation rescues the oncogenic effects of miR-424 in vitro and in vivo.

(A-C) Immunoblot (IB) of STAT3 (A), colony formation in soft agar (B) and SFE (C) in RWPE1 cells following co-transfection with miR-424 or Ctr and siRNA targeting STAT3 (siSTAT3_n2) or control siRNA (siGL3). (D), Schematic of the experimental plan and (lower) immunoblot of STAT3 following knockdown with siRNA_n1 in RWPE1 cells before the engraftment. (E) Representative images of H&E, immunostaining (20X magnification) and IHC scores (% of positive cells). Differences in stain of indicated proteins between siGL3 and siSTAT3 were statistically significant ($p < 0.01$).

List of 323 predicted miR-424 targets in prostate epithelial cells

ABCB8
ABCF1
ABCF2
ACTR2
ACVR2B
ADD2
ADSS
AHCYL2
AHNAK2
ANAPC13
ANGEL1
ANKRD12
ANKRD46
AP1S3
AP2A1
AP2B1
AP3B1
APP
ARFRP1
ARHGAP12
ARHGAP5
ARHGDIA
ARL10
ARL2
ATF6
ATG9A
ATP13A2
ATP13A3
ATXN2
ATXN7L1
ATXN7L3
B4GALT1
BCL7A
BCL9L
BCR
BIK
BLCAP
BMS1
BTBD2
BTG2
BTRC
C10orf54
C11orf24
C11orf45
C14orf126
C14orf37
C1orf190
C20orf29
C9orf100

C9orf102
CAB39L
CAMK2G
CAPRIN1
CARD10
CARM1
CASK
CBFB
CC2D1B
CCDC19
CCND1
CCND2
CCND3
CCNE1
CCNF
CCNG1
CDC25A
CDC37L1
CDC42EP2
CDCA4
CDK6
CHD6
CHMP4B
CHORDC1
CHPT1
CHUK
CLASP1
CLCN3
CLCN6
CLDN12
CLOCK
CMTM4
CNNM2
CNOT6L
CNTNAP1
COBLL1
COPS7B
CRYZL1
CTNND1
CUL2
CYB561
CYP26B1
CYP27B1
CYP2S1
DCTN5
DENR
DNAJC16
DSCR3
EEA1
EFTUD2

EIF5A
ENPP4
ENTPD6
ENTPD7
EPB41L4B
ERAL1
ESRRG
EXT2
FAM123B
FAM54B
FAM81A
FAM91A1
FAT2
FBXW7
FCF1
FGF11
FKBP1A
FKBP1B
FLCN
FLOT2
G6PD
GALNT7
GATA4
GCC1
GCLC
GIT1
GLS
GPATCH8
GYS1
HARS2
HMGA1
HOXA10
HOXC11
HR
HSPG2
IARS
IGF2R
IKBKB
JRK
KBTBD4
KCMF1
KCNN4
KCTD1
KIAA0317
KIAA0895
KIF1B
KIF21A
KIF3B
KLHDC8B
KLHL26

KPNA6
LMO7
LSM11
LYPLA2
MAP2K3
MAPK3
MAPKAP1
MARK4
MFN2
MINK1
MMD
MMP3
MMS19
MRPS2
MS4A7
MTHFR
MYB
MYO1E
NCKIPSD
NEO1
NF1
NFE2L1
NFS1
NMD3
NMT1
NOTCH2
NRBP1
NUCB1
NUDCD3
NUP188
OLR1
OOEP
OS9
PA2G4
PAFAH2
PCMT1
PDIK1L
PDLIM2
PDPR
PER3
PERP
PEX12
PEX13
PHF19
PHF20
PHLDA3
PI4KB
PIP4K2C
PLEKHA1
PLEKHA5

PLEKHB2
PLRG1
PNPLA6
POLL
POLR3F
PPP1R11
PPP1R13B
PPP2R1A
PRDM4
PRKAR2A
PTPN3
PTRF
PURA
RAB10
RAB4B
RANBP3
RAP2C
RAPGEF1
RAPGEF5
RAPGEFL1
RASSF5
RCE1
RFK
RFWD2
RFWD3
RIMS3
RNF138
RNF144B
RNF216
RNF217
RNGTT
RPS6KA3
SAMD10
SCOC
SETD3
SFT2D3
SGSM2
SH3BGR2
SHROOM4
SIDT2
SIRT4
SLC11A2
SLC20A2
SLC22A13
SLC25A22
SLC35A4
SLC35E4
SLC37A2
SLC38A9
SLC39A9

SLC44A2
SLC45A3
SLC7A2
SLC9A1
SLC9A6
SMAP2
SMPD1
SMURF1
SMYD5
SNCG
SNX18
SPAG7
SPRED1
SPRYD3
SPTLC1
SSRP1
SSU72
STIM1
STK33
STK35
SUMO3
SUPT16H
SYT15
TARBP2
TBC1D13
TBC1D19
TBC1D24
TBPL1
TFCP2L1
TMCC1
TMC07
TMEM109
TMEM161B
TMEM43
TMEM55B
TNFSF9
TNIP1
TNS1
TOLLIP
TOM1L2
TOMM34
TPRG1L
TRIOBP
TRIP10
UBAC1
UBE2B
UBE2Q1
UBE3C
UBE4A
UBE4B

UBR3
USP14
USP15
VAC14
VAMP8
VAT1
VCL
VPS33B
VPS4A
VTA1
VTI1B
WBP11
WHSC1
XPO5
XPR1
YTHDC1
ZBTB39
ZDHHC14
ZHX1
ZIK1
ZNF501
ZNF622
ZNRF2
ZYG

Supplemental Table 2

ANAPC13
BTRC
C14orf146
CUL2
FBXW7
FKBP1A
HARS2
KCMF1
KIAA0317
LMO7
PEX13
RCE1
RFWD2
RNF138
RNF144B
RNF217
SMURF1
SUMO3
UBAC1
UBE2B
UBE2Q1
UBE3C
UBE4A
UBE4B
UBR3
USP14
USP15
ZNRF2
RNF216

Supplementary Table 3.

Primers sets used for qRT-PCR

<i>GENE</i>	<i>SEQUENCE</i>
<i>COPI FWD</i>	5'-ACGACCTTTAGCCACATTGT-3'
<i>COPI REV</i>	5'- TAACTCCAGCAATCGCAAAA-3'
<i>ACTIN FWD</i>	5'-ATTGGCAATGAGCGGTTC-3'
<i>ACTIN REV</i>	5'-GGATGCCACAGGACTCCAT-3'
<i>MYC-C FWD</i>	5'-GGTGCTCCATGAGGAGACA-3'
<i>MYC-C REV</i>	5'-CCTGCCTCTTTCCACAGAA-3'
<i>STAT3 FWD</i>	5'-GGAGGAGTTGCAGCAAAAAG-3'
<i>STAT3 REV</i>	5'-GATTCTCTCCTCCAGCATCG-3'
<i>IL6 FWD</i>	5'-CCACACAGACAGCCACTCAC-3'
<i>IL6 REV</i>	5'-TTTCAGCCATCTTTGGAAGG-3'
<i>DDIT4 FWD</i>	5'-GGTTCGCACACCCATTCAAG-3'
<i>DDIT4 REV</i>	5'-TAGGCATGGTGAGGACAGAC-3'
<i>NANOG FWD</i>	5'-CAGTCTGGACACTGGCTGAA-3'
<i>NANOG REV</i>	5'-CTCGCTGATTAGGCTCCAAC-3'
<i>POU5F1 FWD</i>	5'-AGCGATCAAGCAGCGACTAT-3'
<i>POU5F1 REV</i>	5'-TAGCCTGGGGTACCAAAATG-3'
<i>SOX2 FWD</i>	5'-AACCCCAAGATGCACAAC-3'
<i>SOX2 REV</i>	5'-GCTTAGCCTCGTCGATGAAC-3'
<i>ESE3 FWD</i>	5'-TGCAGCATCTGAAGTGGAAC-3'
<i>ESE3 REV</i>	5'-AGGAAGGTGACTGGTGGTTG-3'

Supplemental Table 4

sample_ID	expression profiling	Age	Gleason Score	Grading_G	pT	pN	pM
A5	miR and GEP	70	8	3	3A	0	0
A9	miR and GEP	67	6	2	2A	0	0
CC35	miR and GEP	65	6	2	3A	x	0
CC62	miR and GEP	70	7	3	2C	0	0
CC75	miR and GEP	66	7	3	3B	x	0
CC83	miR and GEP	67	7	3	3A	x	0
D40	miR and GEP	50	7	2	2C	0	0
CC91	miR and GEP	71	7	3	3B	0	0
L12	miR and GEP	65	7	2	2C	0	0
Y48	miR and GEP	65	7	2	3B	x	0
CC17	miR and GEP	63	8	3	3A	0	0
CC87	miR and GEP	70	9	3	3B	0	0
G70	miR and GEP	73	7	2	2B	x	0
P55	miR and GEP	72	7	2	2C	x	0
P60	miR and GEP	64	8	3	2C	0	0
W25	miR and GEP	69	8	3	3A	0	0
W28	miR and GEP	61	6	2	2C	x	0
Y44	miR and GEP	62	6	2	2C	x	0
A3	miR and GEP	67	7	2	2B	0	0
B11	miR and GEP	68	7	2	2C	x	0
B17	miR and GEP	71	7	2	2A	x	0
BB5	miR and GEP	61	7	2	2C	0	0
C25	miR and GEP	65	7	2	3A	0	0
C27	miR and GEP	73	7	2	2A	x	0
L16	miR and GEP	72	7	2	2C	0	0
M26	miR and GEP	61	7	2	2C	x	0
Q70	miR and GEP	62	6	2	2C	x	0
V18	miR and GEP	68	7	2	2C	x	0
Z56	miR and GEP	64	7	2	3A	x	0
AA65	miR and GEP	69	7	2	2C	0	0
AA69	miR and GEP	68	6	2	2C	0	0
B12	miR and GEP	72	6	2	2C	x	0
CC3	miR and GEP	55	7	2	3B	0	0
CC41	miR and GEP	67	7	3	2C	x	0
CC8	miR and GEP	70	6	2	3A	x	0
D36	miR and GEP	73	7	2	3A	x	0
E50	miR and GEP	67	8	3	3A	0	0
G64	miR and GEP	70	9	3	3A	0	0
Y50	miR and GEP	63	7	2	2A	x	0
AA90	miR and GEP	65	7	2	2C	0	0
AA97	miR and GEP	59	7	2	3A	x	0
H75	miR and GEP	70	7	2	2B	x	0
K6	miR and GEP	67	9	3	2C	0	0
P51	miR and GEP	53	8	3	4	1	0
P57	miR and GEP	69	8	3	2C	x	0
X40	miR and GEP	68	6	2	2A	x	0
Z55	miR and GEP	52	6	2	2C	x	0
Z59	miR and GEP	57	6	2	2C	x	0